RESEARCH ARTICLE

WILEY

Solid-state nuclear magnetic resonance and nuclear quadrupole resonance as complementary tools to study quadrupolar nuclei in solids

Patrick M.J. Szell [ID] | David L. Bryce [ID]

Department of Chemistry and Biomolecular Sciences & Centre for Catalysis Research and Innovation, University of Ottawa, Ottawa, ON, Canada

Correspondence
D.L. Bryce, Department of Chemistry and Biomolecular Sciences & Centre for Catalysis Research and Innovation, University of Ottawa, Ottawa, ON, Canada.
Email: dbryce@uottawa.ca

This article is a contribution to the special issue in honor of Alex Bain.

Abstract

Solid-state nuclear magnetic resonance (SSNMR) spectroscopy has largely overtaken nuclear quadrupole resonance (NQR) spectroscopy for the study of quadrupolar nuclei. In addition to information on the electric field gradient, SSNMR spectra may offer additional information concerning other NMR interactions such as magnetic shielding. With continued technological advances contributing to developments such as higher magnetic fields, SSNMR boasts several practical advantages over NQR. However, NQR is still a relevant technique, as it may often be the most practical approach in cases of extremely large quadrupolar coupling constants. Here, we discuss the advantages and disadvantages of SSNMR and NQR spectroscopies, with the quadrupolar halogens serving as examples. The purpose of this article is to serve as a guide on using SSNMR and NQR as complementary tools, covering some of their practicalities, limitations, and experimental challenges.

KEYWORDS
nuclear quadrupole resonance, quadrupolar halogens, quadrupolar nuclei, solid-state nuclear magnetic resonance

1 | INTRODUCTION

Solid-state NMR (SSNMR) spectroscopy has become a widely implemented analytical tool, offering information on chemical, crystallographic, and electronic environments, as well as dynamical information. Due to the nature of SSNMR, it boasts some advantages over diffraction-based techniques, such as the ability to study glasses and other amorphous and heterogeneous systems, host-guest systems, and molecular dynamics and disorder. Although NMR experiments are most routinely applied to spin $I = \frac{1}{2}$ nuclei, such as ^1H and ^{13}C, approximately 75% of the periodic table is composed of quadrupolar nuclei ($I > \frac{1}{2}$). Of course, SSNMR is not limited to spin-$\frac{1}{2}$ nuclei, and there

is an extensive history and literature on the analysis of quadrupolar nuclei by SSNMR.[1] A technique analogous to SSNMR, but performed in the absence of a magnetic field, is nuclear quadrupole resonance (NQR) spectroscopy, which is applicable strictly in the cases of quadrupolar nuclei ($I > \frac{1}{2}$).[2-4] NQR does not require the application of an external magnetic field due to the fact that the quadrupolar interaction perturbs the energy levels of the nuclear spin states, allowing transitions to occur between the resulting nondegenerate energy levels.

Over the course of its evolution, SSNMR has largely overtaken NQR spectroscopy for the investigation of solids. As shown in Figure 1, mentions of SSNMR in the scientific literature have greatly surpassed NQR. In part, this can be attributed to the former's higher sensitivity and the accessibility of spin $\frac{1}{2}$ nuclei, in addition to the higher abundance of information obtained from spin manipulation

In honor of the significant contributions and impact of Alex Bain in the field of nuclear magnetic resonance.
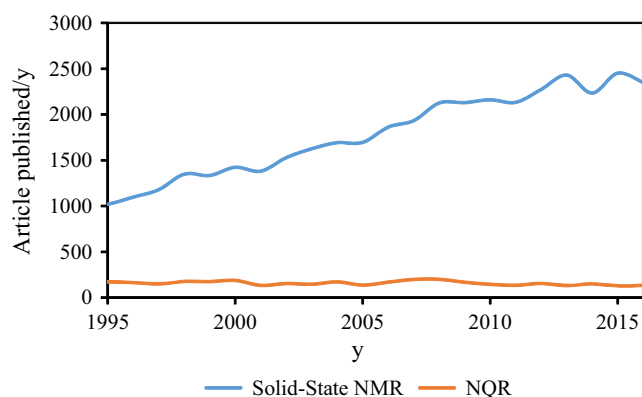
FIGURE 1 Number of Web of Science[70] literature results per year for the queries "Solid-State NMR" and "Nuclear Quadrupole Resonance" in the last 20 years (1995 to 2016)

via advanced multipulse and multidimensional experiments. A key practical advantage to SSNMR experiments is that the spectrum is always predictably roughly centered on the Larmor frequency. Contrarily, in NQR experiments, one may be forced to search over extremely wide spectral windows (tens of MHz or more) to find the resonances in the absence of a priori information on the magnitude of the quadrupolar interaction in a given sample. Additionally, with technological developments, such as high magnetic fields and so-called ultra-fast magic angle spinning rates,[5] SSNMR can be used routinely to obtain information on the chemical shift tensor, quadrupolar coupling tensor, the dipolar coupling tensor, and *J*-coupling.[6] However, NQR is not obsolete, as it can be used to study quadrupolar nuclei with large quadrupole moments, offering comparatively sharp resonances without the need for a stable external magnetic field. This advantage allows NQR to be applied in instances where SSNMR experiments would be difficult to perform, notably in cases when nuclei are subject to very large quadrupolar interactions. At a minimum, NQR can often be used as a complementary tool to SSNMR, allowing for a rapid verification of the quadrupolar coupling parameters. This verification can be particularly advantageous if the SSNMR spectrum results from a subtle interplay between a dominant quadrupolar coupling interaction and a relatively small anisotropic magnetic shielding interaction.

The quadrupolar interaction is the result of coupling between the electric field gradient (EFG) at a nucleus and its quadrupole moment (*Q*). The quadrupolar interaction offers structural information through the distortion of the electronic environment surrounding the nucleus. Several recent papers in the literature have focused on nuclei featuring large quadrupolar interactions and concomitantly broad SSNMR spectral breadths, which are time-consuming to fully acquire. NQR can play a role in these studies, and

one might ask, "under which circumstances should I perform NMR experiments and when should I perform NQR experiments?" Here, we offer a discussion on the use of SSNMR and NQR to study quadrupolar nuclei, first by covering some basic theory, and then by discussing some of the practical aspects of both techniques with emphasis on their advantages and limitations. The focus is solely on powdered samples. As several articles have already offered a complete theoretical treatment of the quadrupolar interaction,[7,8] the theory offered here covers only the fundamentals required to understand the practical differences between NQR and SSNMR spectroscopies. This *Concepts* article will serve as a complement to the comparisons between SSNMR and NQR available in the literature,[9] including elegant and insightful work by Alex Bain.[10,11]

2 | REVIEW OF BASIC THEORY

The quadrupolar interaction arises as a result of the coupling between the nuclear quadrupole moment (*Q*) and the electric field gradient (EFG) tensor. The quadrupole moment arises due to an asymmetrical charge distribution within the nucleus itself, whereas the EFG is the second derivative of the electrostatic potential at the nucleus. The EFG is represented by a traceless second-rank tensor, and in its principal axis system, its magnitude can be expressed by three principal components: V_{11}, V_{22}, and V_{33}. By convention, the largest component of the tensor is V_{33}, such that $|V_{33}| \geq |V_{22}| \geq |V_{11}|$. These magnitudes can also be conveniently described by the quadrupolar coupling constant, C_Q (Equation 1), and the asymmetry parameter, η (Equation 2).

$$C_Q = \frac{eV_{33}Q}{h} \qquad (1)$$

$$\eta = \frac{V_{11} - V_{22}}{V_{33}} \qquad (2)$$

Here, *e* is the fundamental charge (expressed in C), V_{33} is expressed in atomic units, *Q* is the quadrupole moment (expressed in fm²), and *h* is Planck's constant (expressed in J s). The full details of dealing with the units of Equation 1 have been discussed previously.[12] The value of C_Q indicates the magnitude of the quadrupolar interaction, whereas η describes the axial symmetry of the tensor. In cases of high symmetry, such as the cubic structures of alkali salts (eg, NaCl), the EFG at these nuclei would be very small, owing to the fact that all principal components are identical ($V_{11} = V_{22} = V_{33} = 0$).[13] In contrast, for compounds with asymmetric charge distribution about a nucleus, such as a nucleus with one covalent bond, the resulting EFG would be much larger. Consequently, the quadrupolar interaction

is expected to be large, which varies as a function of the value of Q for a given nuclide. The interpretation of the quadrupolar coupling tensor can become quite detailed, and the reader is referred to an excellent *Concepts* article by Autschbach et al.[14]

In SSNMR, the influence of the quadrupolar interaction on the spectrum (in particular its breadth) will depend on the size of the quadrupolar interaction. In the cases where the quadrupolar interaction is small, the total NMR Hamiltonian (H_{NMR}) can be approximated as a perturbation on the Zeeman Hamiltonian (H_{Zeeman}), given in Equation 3:

$$H_{NMR} = H_{Zeeman} + H_{RF} + H_J + H_{DC} + H_Q \quad (3)$$

Here, we refer to the Hamiltonians of the radiofrequency interactions (H_{RF}), the *J*-coupling interaction (H_J), the dipolar coupling interaction (H_{DC}), and the quadrupolar coupling interaction (H_Q). Second-order perturbation theory has proven to be quite successful in the interpretation of the SSNMR spectra of quadrupolar nuclei.[8,10] However, there are limits to its applicability, namely in the cases where the quadrupolar interaction becomes dominant.[15,16] It has been proposed that for perturbation theory to be applied reliably, the ratio of the Larmor frequency, ν_L (Equation 4), and the quadrupolar frequency, ν_Q (Equation 5), should be above 10.[15]

$$\nu_L = \frac{\gamma B_0}{2\pi} \quad (4)$$

$$\nu_Q = \frac{3C_Q\sqrt{1 + \frac{\eta^2}{3}}}{2I(2I-1)} \quad (5)$$

In Equation 4, γ refers to the gyromagnetic ratio of the nucleus and B_0 refers to the external magnetic field strength, whereas in Equation 5, I refers to the spin quantum number of the nucleus. Note that the third-order correction has been shown to be zero by Alex Bain.[17] When performing SSNMR experiments on half-integer spin quadrupolar nuclei, it is generally suggested to go to higher applied magnetic fields, as the width of the central-transition (CT) NMR spectrum is inversely proportional to ν_L, shown in Equation 6.[18,19]

$$\Delta\nu_{CT} = \left(\frac{25 + 22\eta + \eta^2}{144}\right)\left[\frac{(3C_Q)^2}{((2I)(2I-1))^2}\right]\left[\frac{I(I+1) - \frac{3}{4}}{\nu_L}\right] \quad (6)$$

However, sufficiently strong magnetic fields may either not be available or not be practical, in which case the absence of a magnetic field can be beneficial for the analysis of nuclei subject to large quadrupolar interactions.

As pure NQR is performed in the absence of a magnetic field, the Zeeman interaction term can be dropped from Equation 3, giving the basic Hamiltonian for NQR in Equation 7:
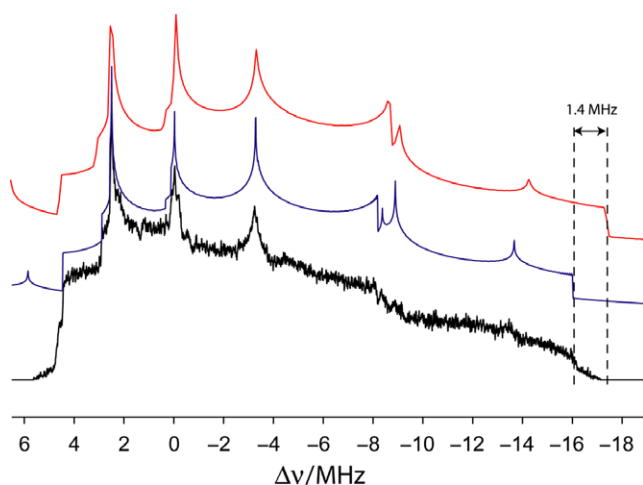
$$H_{NQR} = H_{RF} + H_J + H_{DC} + H_Q \quad (7)$$

Here, the terms are the same as for Equation 3; however, the quadrupolar interaction is generally the dominant term. As the H_J and H_{DC} terms are not dropped, however, they do contribute to the NQR line shape, usually in the form of line broadening.[20] As a consequence of Equation 1 and Equation 5, when nuclei with small quadrupole moments are analyzed with NQR, such as ^{2}H ($Q = 2.860(15)$ mb)[21] and ^{6}Li ($Q = -0.808$ mb),[21] the expected NQR frequencies are very low (kHz range).[22]

The energy level diagram pertaining to the analysis of an arbitrary spin-3/2 nucleus by SSNMR and NQR is presented in Figure 2. In cases where ν_Q approaches zero, the energy levels are dictated by the Zeeman interaction and the corresponding NMR spectrum would simply reflect the Zeeman splitting (Figure 2A). Upon the introduction of a weak quadrupolar interaction ($\nu_L/\nu_Q > 10$), first-order (Figure 2B) and second-order (Figure 2C) perturbations are applied to the energy levels. In the case of a spin-3/2 nucleus exhibiting a large quadrupolar interaction relative to the Zeeman interaction ($\nu_L/\nu_Q < 10$), the energy levels shift substantially from the high-field regime (Figure 2D) and perturbation theory is no longer reliable. In the absence of a magnetic field, these energy levels collapse to two degenerate states, the $\pm1/2$ state and the $\pm3/2$ state (Figure 2E). In the pure NQR spectrum of a spin-3/2 nucleus, the $\pm1/2 \rightarrow \pm3/2$ transition is observed, with the energy levels and resulting frequency dictated by the quadrupolar interaction. Although only one NQR transition is observed for $I = 3/2$ nuclei, more generally the number of NQR transitions varies as a function of the spin quantum number. For instance, for a spin 5/2 nucleus, the observed transitions are typically $\pm1/2 \rightarrow \pm3/2$ and $\pm3/2 \rightarrow \pm5/2$. It is to be noted that the overtone transition, $\pm1/2 \rightarrow \pm5/2$, can sometimes be observed.[23,24] As the Boltzmann spin population is proportional to the difference in the energy levels, the sensitivity of NQR experiments generally increases with the magnitude of the QI. However, in SSNMR experiments, spectral widths increase with the magnitude of the QI, leading to a spread of the inherent signal over a broader frequency range and therefore an effectively lower signal-to-noise ratio. A higher magnetic field results in a narrower NMR spectrum and a gain in sensitivity, overall being favorable for the analysis of quadrupolar nuclei by SSNMR.

Although perturbation theory certainly has its uses, it does not hold in the cases of large quadrupolar interactions ($\nu_L/\nu_Q < 10$), and an exact theory must be applied in order to accurately simulate the resulting spectra.[15,24] The QUadrupole Exact SofTware (QUEST)[24] has been developed in
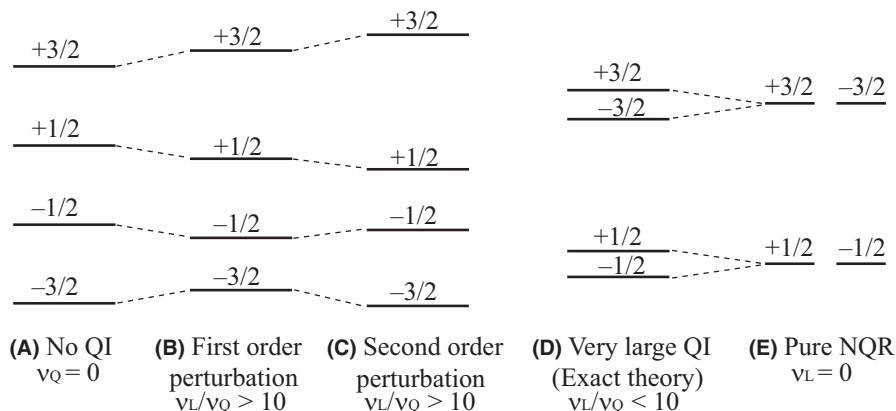
FIGURE 2 Energy level diagram (not to scale) for a spin $I = 3/2$ nucleus subjected to the Zeeman interaction A, with a first-order perturbation from the quadrupolar interaction B, with first- and second-order perturbations from the quadrupolar interaction C, with a large quadrupolar interaction relative to the Zeeman interaction D, and a quadrupolar interaction without Zeeman splitting E. ν_Q refers to the quadrupolar frequency and ν_L refers to the Larmor frequency. The ordering of the spin states on the left depends on the sign of the gyromagnetic ratio

3 | USING A SSNMR SPECTROMETER FOR NQR SPECTROSCOPY

Although a proper NQR spectrometer is evidently the most appropriate for NQR experiments, a modern SSNMR spectrometer can double as a NQR spectrometer in many cases. Due to the resemblances in the experiments and hardware requirements, one can operate an NMR probe in the absence of a magnetic field and obtain the NQR transitions. The general limiting factors are first in generating the desired radiofrequencies and secondly in acquiring the signal through the NMR hardware. Most modern SSNMR spectrometers, for instance, the Bruker Avance III console in our laboratory, will have a wide operational frequency range for the X nucleus and a relatively limited range for the $^{1}H/^{19}F$ channel. The frequency ranges for the signal generating unit and the amplifier typically span hundreds of MHz, with the ranges varying to suit the strength of the applied magnetic field. However, NMR spectrometers may be limited to generating frequencies above 5 MHz, and a low-frequency NQR spectrometer[25] would be advantageous to perform experiments at lower frequencies. When using your SSNMR spectrometer for NQR, considerations should be made to use the appropriate preamplifier and filters, to ensure that output or input frequencies are not being attenuated.

Perhaps the most restrictive criterion for performing NQR on a SSNMR spectrometer is the tuning range of the NMR probe. A commercial NMR probe is typically manufactured to tune to the Larmor frequency for a range of nuclei, such as ^{15}N through ^{31}P, with a specific applied magnetic field in mind. Consequently, the tuning range of

FIGURE 3 $^{79/81}Br$ NMR spectrum of $CaBr_2$ acquired at 4.7 T, showing the difference between simulations using an exact Hamiltonian diagonalization (blue) and second-order perturbation theory (red). (Figure taken from *Solid State Nucl. Magn. Reson.* **2012**, *45-46*, 36-44.[24] Used with permission.)

our laboratory to treat the quadrupolar interaction exactly, allowing one to extract spectral parameters from NMR and NQR spectra accurately over the full range shown in Figure 2. Shown in Figure 3 is an example of the importance of using exact theory when dealing with large quadrupolar interactions relative to the Zeeman interaction.[24] Ultra-wideline $^{79/81}Br$ SSNMR spectroscopy was performed on solid powdered $CaBr_2$ in an applied magnetic field of 4.7 T, with a final CT spectral width of approximately 20 MHz. A 1.4 MHz discrepancy is seen between second-order perturbation theory and exact theory on the right edge of the spectrum.

such a probe is customized according to the magnetic field strength in which it was meant to operate. However, one is not restricted to use the NMR probe intended for a specific magnetic field, as the only essential aspect is being able to tune in the range of the anticipated NQR frequency. Where a wide tuning range is needed, such as for ^{127}I NQR experiments, building a dedicated single-channel solenoid NQR probe can offer the required flexibility. This can be accomplished without most of the space restraints associated with building an NMR probe, and there are various designs available in the literature.[26,27] Additionally, with access to an automatic tuning and matching probe,[28] NQR experiments can be performed without the agony associated with staring at noise while continuously retuning the probe to search for NQR transitions.
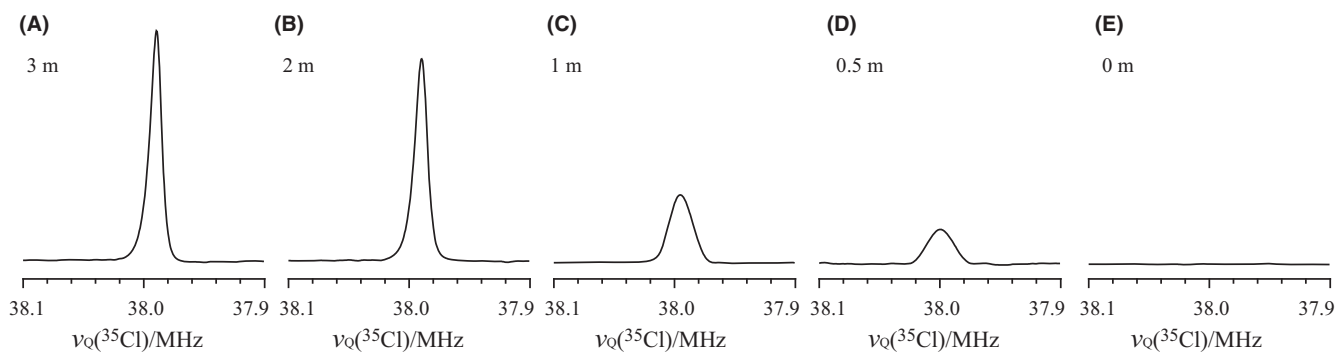
Once the appropriate hardware setup has been prepared, the desired frequency must be generated from the amplifiers. From there, the frequency offset is varied, step by step, in order to find the NQR transition(s). Although the experiment can be performed using direct one-pulse excitation, a spin-echo pulse sequence can also be used to minimize the probe ringing, which is especially useful at low frequencies (ν_Q < 20 MHz). Prior to commencing the experiment, the pulse lengths should be optimized on a sample with a known NQR frequency, with the goal of maximizing the signal intensity. The size of the frequency steps should also be chosen appropriately, as taking large steps can result in "missing" the signal, whereas taking small steps can become overly time-consuming. The size of the frequency steps can be optimized using the same sample by changing the offset until the signal can barely be observed. A typical step size used in our laboratory is 250 kHz. In cases where the nucleus of interest is dilute and/or the amount of sample available is small, smaller frequency steps can be advantageous to maximize the chances of observing the NQR signal(s). Shaped pulses have been shown to be useful in NQR spectroscopy, maximizing the excitation bandwidths of the pulses and thereby reducing the number of steps required.[16]

One of the inherent disadvantages of performing NQR using a SSNMR spectrometer is the possible presence of a stray magnetic field from the nearby superconducting magnet. Although modern shielded magnets greatly reduce the size and strength of the stray magnetic field, stray fields are nevertheless an important consideration as the presence of a magnetic field will induce an undesirable Zeeman splitting or spectral broadening. Therefore, the NQR experiment should be performed as far away from the NMR magnet as possible, to avoid any interactions with the stray magnetic field. Otherwise, the result is generally a broadening in the NQR line shape due in part from the magnetic field inhomogeneity, rendering it more difficult to observe. To demonstrate this effect, we have performed ^{35}Cl NQR experiments on tetrachloroterephthalonitrile (ν_Q ~ 38 MHz), using a Bruker Avance III console operating near an unshielded Oxford Instruments 200 MHz NMR magnet. We have varied the distance between the probe head and the center of the bore of the superconducting magnet in several steps: 3 m, 2 m, 1 m, and 0.5 m away, and inside the magnet. Shown in Figure 4 is the result of each experiment, with a clear reduction in the signal-to-noise ratio and a 10 kHz frequency shift of the resonance between spectra (A) and (D).

4 | FURTHER PRACTICALITIES, LIMITATIONS, AND EXPERIMENTAL CHALLENGES

As mentioned above, both SSNMR and NQR have their particular advantages. SSNMR offers insights into both the chemical shift tensor and the quadrupolar coupling tensor.

(A) 3 m **(B)** 2 m **(C)** 1 m **(D)** 0.5 m **(E)** 0 m

38.1 38.0 37.9 $\nu_Q(^{35}Cl)$/MHz   38.1 38.0 37.9 $\nu_Q(^{35}Cl)$/MHz   38.1 38.0 37.9 $\nu_Q(^{35}Cl)$/MHz   38.1 38.0 37.9 $\nu_Q(^{35}Cl)$/MHz   38.1 38.0 37.9 $\nu_Q(^{35}Cl)$/MHz

FIGURE 4 ^{35}Cl NQR spectra of tetrachloroterephthalonitrile acquired at room temperature on a Bruker Avance III console near a 200 MHz (4.7 T) unshielded Oxford Instruments magnet. The NQR experiment was performed at a distance of A, 3 meters (~0.3 mT), B, 2 meters (~0.7 mT), C, 1 meter (~4.0 mT), D, 0.5 meters (>5.0 mT), and E, 0 meters (inside the magnet), in order to demonstrate the effect of stray magnetic field on the NQR line shape. Each spectrum was acquired with a Hahn echo, 512 transients, and a 1 s recycle delay. Stray magnetic field strengths and distances are approximate

A set of NMR parameters can be extracted by iteratively fitting the experimental NMR spectrum using software such as QUEST[24] for exact simulations or WSolids[29] for second-order perturbation simulations. However, the acquisition of SSNMR spectra of quadrupolar nuclei is dictated by the receptivity of the nucleus, the line widths, and availability of high magnetic fields, to name a few considerations.[19] In comparison, pure NQR is relatively straightforward to perform using an NMR console, but as it is measured through the magnetic induction from the nuclear magnetic moments,[30] the sensitivity is also dependent on the receptivity of the nucleus. In the case of a spin-3/2 nucleus, the pure NQR spectrum would yield the product of the C_Q and η, ν_Q (Equation 5). In the cases of $I > 3/2$ and $I = 1$, obtaining more than one NQR transition would offer the values of both C_Q and η. However, pure NQR offers no information on magnetic field dependent (in frequency units) observables, such as the chemical shift tensor, and thus, SSNMR is inherently richer in information.

As mentioned earlier, in SSNMR, the second-order quadrupolar interaction scales inversely with the strength of the applied magnetic field. Consequently, higher magnetic fields are desirable for the analysis of quadrupolar nuclei, as they not only increase the sensitivity of the experiment, but also yield narrower quadrupolar line shapes. SSNMR analysis can be performed either under spinning conditions or under static conditions. In the case of analyzing a quadrupolar nucleus under spinning conditions, the most popular technique is magic angle spinning (MAS), where the sample is spun about the magic angle (54.74°)[31] with respect to the magnetic field, at a rate that would exceed the CT spectral width. Additionally, several MAS pulse sequences allow for the measurement of dipolar coupling and CSA under spinning conditions.[32] Alternative spinning methods include double rotation NMR (DOR),[33,34] where the first- and second-order quadrupolar interactions can be averaged by spinning both about the magic angle and an angle of 30.56° with respect to the magic angle. Other spinning methods exist, such as variable-angle spinning[35] and dynamic angle spinning,[36] offering alternative methods of analyzing quadrupolar nuclei. However, a nucleus exhibiting large quadrupolar interactions would either require impractically fast spinning speeds (perhaps on the order of MHz) or the deconvolution of unresolved spinning sidebands from the isotropic peaks. Multiple quantum magic angle spinning (MQMAS) is another alternative, which combines MAS with a multipulse sequence in order to obtain high-resolution spectra.[37] Additionally, new pulse sequences with the combination of fast MAS and indirect detection offer several advantages compared to the aforementioned techniques.[38] It is also possible to gain information on the C_Q indirectly through the SSNMR observation of neighboring nuclei. Fitting the resulting MAS line shapes can yield not only the value of C_Q, but has also been useful in determining the absolute sign of C_Q.[39]

Despite the applicability of MAS, SSNMR analysis of quadrupolar nuclei under static conditions is technologically more straightforward, while still offering an abundance of information. Signal enhancement techniques and advances in pulse sequences have allowed for the acquisition of very broad static NMR spectra. There is a wealth of information concerning signal enhancement of quadrupolar nuclei, perhaps with the most important being the Carr-Purcell-Meiboom-Gill (CPMG) pulse sequence applied to quadrupolar nuclei.[40] The combination of signal enhancement techniques, shaped pulses (ie, WURST pulses[41]), and variable offset cumulative spectral acquisition (VOCS)[42] enable "ultra wideline" SSNMR.[43,44] These techniques have made it possible to acquire spectra spanning hundreds of kHz and even several MHz.

In Figure 5A, the ultra-wideline ^{35}Cl solid-state NMR spectra of tetrachloroterephthalonitrile, acquired at field strengths of 35.2 T and 21.1 T using WURST-QCPMG are presented.[45] The central-transition ^{35}Cl NMR spectrum spans roughly 5.5 MHz at 35.2 T and 9 MHz at 21.1 T, requiring the acquisition of 14 subspectra near 35.2 T by sweeping the magnetic field, and 20 subspectra at 21.1 T using multiple transmitter offsets. The resulting spectrum at 21.1 T was fitted with QUEST,[24] yielding the values of C_Q, η, and δ_{iso} from a single 1D spectrum for two crystallographically distinct chlorine sites. The pure ^{35}Cl NQR spectrum of the same compound is presented in Figure 5C, with line widths of approximately 10 kHz. Only the quadrupolar product frequencies, ν_Q, are available from this spectrum. In this example, NQR was used as a complementary tool to SSNMR, allowing for the verification of the quadrupolar coupling parameters obtained from SSNMR.[45] Whereas the SSNMR spectrum took roughly 8 hours to acquire at 21.1 T, the NQR experiments took just 20 minutes to perform, but only with the knowledge of where to search for the resonances gained first from the SSNMR experiment.

Although it may be theoretically possible to acquire the SSNMR spectra of compounds exhibiting arbitrarily large quadrupolar interactions, in practice, there are limitations. A large quadrupolar interaction may result in CT broadening over many MHz or even over hundreds of MHz, precluding the acquisition of any signal. In Figure 6, we present a comparison between simulated SSNMR and NQR spectra of 1,4-dichlorobenzene (p-$Cl_2C_6H_4$), 1,4-dibromobenzene (p-$Br_2C_6H_4$), and 1,4-diiodobenzene (p-$I_2C_6H_4$). In each case, the spectra were simulated using an applied magnetic field strength of 21.1 T using QUEST[24] and literature quadrupolar frequency values, which are summarized in Table 1. The satellite transitions were included in the
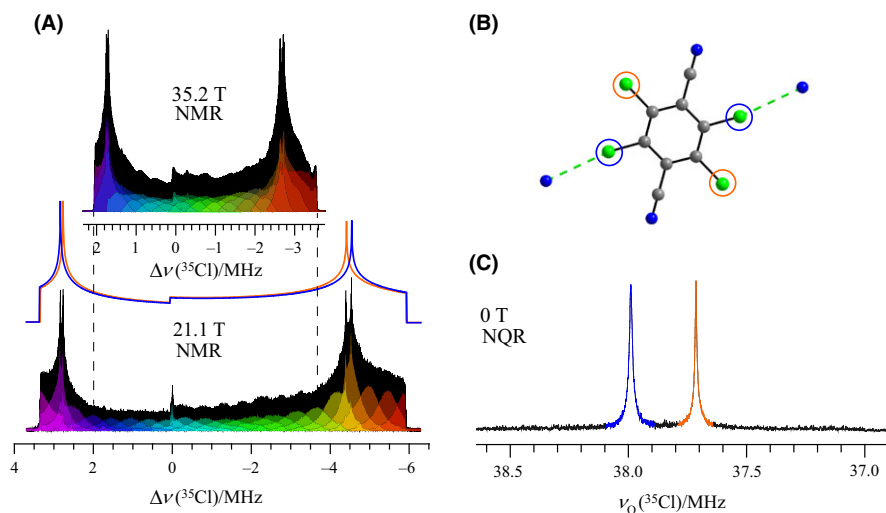
FIGURE 5 A, ^{35}Cl solid-state NMR spectrum of tetrachloroterephthalonitrile acquired at 35.2 T (upper) and 21.1 T (lower). At 35.2 T, a total of 14 subspectra were acquired, whereas at 21.1 T, a total of 20 subspectra were acquired (shown in color) and co-added in the frequency domain to yield the full spectrum (black). The QUEST simulated spectra for each of the two crystallographically distinct sites at 21.1 T are shown in blue and orange. B, The crystal structure of tetrachloroterephthalonitrile, showing the distinct chlorine sites in blue and orange. C, The ^{35}Cl NQR spectrum of tetrachloroterephthalonitrile. The blue and orange peaks correspond to the respective colored sites shown in the structure above. Experimental parameters for the 21.1 T and NQR acquisitions can be found in the original article[45]

simulations, with the area corresponding to the central transitions filled in with color. Much like the case in Figure 5A, the line widths of the central transition of $^{35/37}$Cl (Q (^{35}Cl) = −81.65(80) mb, $Q(^{37}$Cl) = −64.35(64) mb)[21] covalently bonded to carbon are manageable by SSNMR[45,46] and also provide information on the chemical shift. As is immediately apparent however, the line widths of the central transitions of $^{79/81}$Br ($Q(^{79}$Br) = 313(3) mb, Q (^{81}Br) = 262(3) mb)[21], and ^{127}I ($Q(^{127}$I) = −696(12) mb)[21] covalently bonded to carbon become prohibitively large, spanning hundreds of MHz. In contrast, the NQR signals are orders of magnitude sharper.

In the case of ^{127}I, which is a spin-5/2 nucleus, the acquisition of both pure NQR transition frequencies

($\pm1/2 \leftrightarrow \pm3/2$, ν_1; $\pm3/2 \leftrightarrow \pm5/2$, ν_2) yields the same information on the quadrupolar coupling parameters as would SSNMR, that is, independent values of C_Q and η. In order to perform the SSNMR experiment, an impractically high magnetic field strength would be required. For instance, using the data presented in Table 1 on p-I$_2$C$_6$H$_4$, the ^{127}I CT spectral width can be reduced from approximately ~164 MHz at 21.1 T to ~42 MHz at 300 T. In contrast, NQR would require searching for transitions over tens of MHz. Therefore, in this case, performing the pure NQR experiment is the only practical form of RF spectroscopy.

Where sample size and receptivity are not an issue, a principal drawback of NQR lies in finding the NQR transitions over a potentially large frequency range. Knowing the
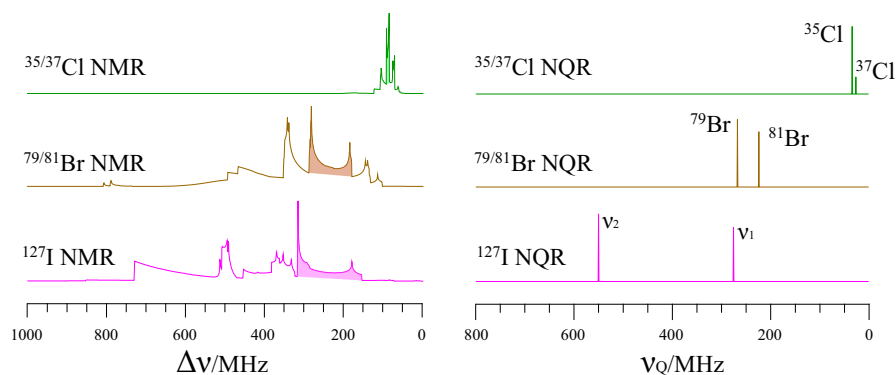
FIGURE 6 Simulated $^{35/37}$Cl, $^{79/81}$Br, and ^{127}I SSNMR spectra (left; B_0 = 21.1 T) and corresponding NQR spectra (right) of powdered p-Cl$_2$C$_6$H$_4$, p-Br$_2$C$_6$H$_4$, and p-I$_2$C$_6$H$_4$. Experimental quadrupolar coupling data are summarized in Table 1. The highlighted regions of the SSNMR spectra denote the central transitions. For the ^{127}I spectra, only one site was used in the simulation (C_Q = 1834.7 MHz, η = 0.0477), with ν_1 corresponding to the $\pm1/2 \leftrightarrow \pm3/2$ transition and ν_2 corresponding to the $\pm3/2 \leftrightarrow \pm5/2$ transition. All spectra were simulated using an exact Hamiltonian diagonalization in QUEST

TABLE 1 Experimental quadrupolar coupling constants (C_Q), asymmetry parameters (η), and NQR frequencies (v_Q) for the $^{35/37}$Cl, $^{79/81}$Br, and ^{127}I nuclei in p-Cl$_2$C$_6$H$_4$, p-Br$_2$C$_6$H$_4$, and p-I$_2$C$_6$H$_4$, respectively, obtained from the literature

Compound	C_Q/MHz	η	v_Q/MHz	References
p-Cl$_2$C$_6$H$_4$	*53.9 $\pm$ 0.2* (^{37}Cl) *68.5 $\pm$ 0.2* (^{35}Cl)	0.075 $\pm$ 0.002[a]	*26.98* (^{37}Cl) 34.25 (^{35}Cl)	V. Rehn[71]
p-Br$_2$C$_6$H$_4$	*448.2 $\pm$ 0.5* (^{81}Br) *535.5 $\pm$ 0.5* (^{79}Br)	0.045 $\pm$ 0.002[b,i]	223.8 (^{81}Br) 267.9[ii] (^{79}Br)	i P. Bucci et al.[72] ii G.W. Ludwig[65]
p-I$_2$C$_6$H$_4$	1834.7 $\pm$ 1.0[c] 1839.4 $\pm$ 1.0[c]	0.0477 $\pm$ 0.0040[c] 0.0365 $\pm$ 0.0050[c]	275.89 $\pm$ 0.15 (v_1) 550.16 $\pm$ 0.30 (v_2) 276.31 $\pm$ 0.15 (v_1) 551.68 $\pm$ 0.30 (v_2)	G.W. Ludwig[65]

The italicized numbers have been derived from the experimental data.

[a]Measured using the NQR field frequency method.

[b]Measured using Zeeman-perturbed NQR.

[c]The multiplicity of the C_Q & η values has been attributed to the presence of two crystal phases by Schawlow,[73] as there is only one iodine site in the asymmetric unit.[74]

coordination sphere surrounding the nuclide of interest, in addition to knowledge of literature results for analogous compounds, can dramatically reduce the frequency range to be searched. However, in the cases where possible C_Q values can span a wide range, such as covalently bonded bromine (300 to 600 MHz, ^{81}Br) and iodine (1600 to 2100 MHz, ^{127}I),[2,45,47,48] finding the NQR transitions without an autotuning probe can become a herculean task. For instance, scanning a frequency range of just 10 MHz using 250 kHz steps every 5 minutes would require 3 hours and 20 minutes of continuous effort. Several techniques have been implemented to help get around these issues, such as ultra-broadband electronics[49] and frequency swept pulses,[16] which allow for larger frequency steps.

NQR is commonly performed on nitrogen-14 ($I = 1$) and has been shown to be a potentially effective technique for routine analysis in the fields of explosives[50,51] and pharmaceuticals.[52] As a result of its moderate quadrupole moment ($Q(^{14}N) = 20.44(3)$ mb),[21] and lack of a central transition, ^{14}N SSNMR can be experimentally challenging to perform due to the first-order quadrupolar broadening. Nevertheless, ^{14}N has been the subject of many SSNMR investigations, with advances reported in overtone spectroscopy[53-55] and ultra-wideline ^{14}N SSNMR.[56-58] Although SSNMR is inherently richer in information and more sensitive, the instrumental simplicity gives ^{14}N NQR the practical advantage of being portable and applicable at the site of sample collection. However, as the ^{14}N NQR frequencies are typically in the hundreds of kHz to MHz regime, sensitivity can be problematic.

We have discussed NQR in terms of acquiring a single one-dimensional spectrum for a powdered sample in the absence of a magnetic field. As mentioned previously, one of the limitations of pure one-dimensional NQR of spin-3/2 nuclei is the inability to provide independent values of η and C_Q. However, several NQR techniques allow for the extraction of both η and C_Q from a single NQR transition. Nutation NQR is perhaps the most straightforward to perform, as it can be done using a standard NMR probe without any additional modifications.[59,60] Nutation NQR is implemented as a two-dimensional experiment, where a series of one-dimensional spectra are acquired with incremented pulse lengths. This experiment relies on the dependence of the nutation frequency on the angle between the quadrupolar tensor and the radiofrequency coil axis, allowing for an estimation of η from the line shape of the sheared 2D spectrum. Due to the long pulse lengths and the requirement for high power, one of the drawbacks of nutation NQR is the RF heating, which can result in a loss of resolution.[59] This issue can be mitigated either by having a longer recycle delay, or a device that maintains the sample temperature. Alternatively, Zeeman-perturbed NQR is one of the earlier methods of extracting η and C_Q from NQR transitions using weak magnetic fields.[61] Although many additional experiments exist, a full review of experimental techniques is beyond the scope of this article.

The temperature dependence of the quadrupolar interaction, and therefore the NQR frequency, has long been a subject of interest.[62,63] It is important to consider the temperature when reproducing literature results, as oftentimes NQR frequencies are reported at liquid nitrogen temperature (77 K). The origin of this effect can greatly vary according to the nature of the sample; however, it is most often attributed to molecular vibrations, librations, other forms of dynamics, or even changes in volume.[63]

While we have limited the discussion to crystalline samples, it is worth mentioning that both SSNMR and NQR are known to be powerful tools for the analysis of samples with disorder or low crystallinity,[64] which can be otherwise troublesome to analyze by diffraction-based techniques. The signal afforded from these techniques can be used to extract parameters related to the structure, such as

internuclear dipolar coupling in the case of SSNMR. The line shapes can be fit to model the disorder present in the sample,[65] which is typically manifested through broadening of line shapes. For quadrupolar nuclei, the combination of both SSNMR and NQR can be used to probe the distribution in the QI. In certain cases, NQR resonances can be broadened to span hundreds of kHz, and even several MHz,[66] in which case frequency swept pulses can be beneficial to decrease experimental time.[16]

When performing ultra wideline SSNMR or even NQR, it is important to consider overlap arising from crystallographically distinct sites,[67] overlap from other nuclides, and possible interference from nearby radio transmissions.[68] For instance, while acquiring ultra wideline ^{35}Cl SSNMR spectra at 21.1 T ($\nu_L = 88.2$ MHz), samples that were packed in zirconium rotors produced large ^{91}Zr signals ($\nu_L = 83.7$ MHz), inconveniently overlapping with singularities at -4.5 MHz on the ^{35}Cl spectrum. This problem can easily be circumvented by instead packing the samples in glass tubes. Although it is not noticeable in Figure 5 as a result of the large signal intensity from the sample of interest, radio interference is observed in the +2 MHz region, which corresponds to the local radio stations (~90 MHz). Another issue that has been observed experimentally is the lack of power linearity of the amplifiers. Over a large frequency range, the power output of the amplifier may change subtly. These subtle changes in power output can lead to distortions in the final spectrum. Anisotropy in the spin-lattice and spin-spin relaxation times may also contribute to the distortion of an ultra wideline SSNMR spectrum. Additionally, the Boltzmann population of the spin states may vary across broad spectra, which may further contribute to spectral distortions and lead to a stronger signal intensity at higher frequencies.

Although several methods are available to extract the quadrupolar coupling parameters mathematically from NQR spectra,[69] iteratively fitting the spectra using software is also straightforward. QUEST is available for simulating NQR spectra based on the spin quantum number and the values of η and C_Q.[24]

5 | CONCLUDING REMARKS

Both SSNMR and NQR are valuable tools for the analysis of compounds containing quadrupolar nuclei. Here, we have discussed some of the advantages and disadvantages of both techniques, with the quadrupolar halogens serving as examples. Although the advent of higher magnetic fields and new pulse techniques makes SSNMR a more versatile technique, the presence of very large quadrupolar interactions can hinder its application, with NQR being in some cases the RF spectroscopy of choice. We have discussed some of the practical aspects related to how a SSNMR console can double as a NQR spectrometer, along with some of the associated experimental challenges. Although SSNMR is inherently richer in information, it is clear that a combination of both techniques is the best approach, particularly for nuclei subject to strong quadrupolar interactions, as one technique can help to compensate for the shortcomings of the other.

ORCID

Patrick M.J. Szell https://orcid.org/0000-0002-3185-9892
David L. Bryce http://orcid.org/0000-0001-9989-796X

REFERENCES

1. Ashbrook SE, Duer MJ. Structural Information from Quadrupolar Nuclei in Solid State NMR. *Concepts Magn Reson Part A*. 2006;28A:183-248.
2. Lucken EAC. *Nuclear Quadrupole Coupling Constants*. London: Academic Press Inc.; 1969.
3. Grechishkin VS. Nuclear quadrupole resonance. *Usp Fiz Nauk*. 1959;69:189-216.
4. Smith JAS. Nuclear quadrupole resonance spectroscopy. *J Chem Educ*. 1971;48:39-48.
5. Pandey MK, Hashi K, Ohki S, Nishijima G, Matsumoto S, Noguchi T, et al. 24 T high-resolution and sensitivity solid-state NMR measurements of low-gamma half-integer quadrupolar nuclei ^{35}Cl and ^{37}Cl. *Anal Sci*. 2016;32:1339-1345.
6. Jakobsen HJ, Bildsøe H, Brorson M, Wu G, Gor'kov PL, Gan Z, et al. High-Field ^{17}O MAS NMR Reveals $^1J(^{17}O-^{127}I)$ with its Sign and the NMR Crystallography of the Scheelite Structures for $NaIO_4$ and KIO_4. *J Phys Chem C*. 2015;119:14434-14442.
7. Bain AD. NMR quadrupole Liouvillians for arbitrary spin: exact symbolic expressions and perturbation solutions. *Concepts Magn Reson*. 2013;42A:45-58.

8. Bain AD. The NMR of quadrupolar nuclei. Relationship between exact and perturbation solutions for spin 3/2. *Chem Phys Lett*. 2012;531:267-271.

9. Lee YK. Spin-1 nuclear quadrupole resonance theory with comparisons to nuclear magnetic resonance. *Concepts Magn Reson Part A*. 2002;14:155-171.

10. Bain AD. Quadrupole interactions: NMR, NQR, and in between from a single viewpoint. *Magn Reson Chem*. 2017;55: 198-205.

11. Bain AD, Khasawneh M. From NQR to NMR: the complete range of quadrupole interactions. *Concepts Magn Reson*. 2004;22A:69-78.

12. Adiga S, Aebi D, Bryce DL. EFGShield – A program for parsing and summarizing the results of electric field gradient and nuclear magnetic shielding tensor calculations. *Can J Chem*. 2007;85:496-505.

13. Mestechkin MM. Electric field gradient in cubic and other ionic crystals. *J Phys Condens Matter*. 1995;7:611-623.

14. Autschbach J, Zheng S, Schurko RW. Analysis of electric field gradient tensors at quadrupolar nuclei in common structural motifs. *Concepts Magn Reson*. 2010;36A:84-126.

15. Widdifield CM, Bain AD, Bryce DL. Definitive solid-state $^{185/187}$Re NMR spectral evidence for and analysis of the origin of high-order quadrupole-induced effects for $I = 5/2$. *Phys Chem Chem Phys*. 2011;13:12413-12420.

16. Rossini AJ, Hamaed H, Schurko RW. The application of frequency swept pulses for the acquisition of nuclear quadrupole resonance spectra. *J Magn Reson*. 2010;206:32-40.

17. Bain AD. A simple proof that third-order quadrupole perturbations of the NMR central transition of half-integral spin nuclei are zero. *J Magn Reson*. 2006;179:308-310.

18. Amoureux JP, Fernandez C, Granger P. Interpretation of quadrupolar powder spectra: static and MAS experiments. (Tutorial Session). In: Granger P, Harris RK, eds. *Multinuclear Magnetic Resonance in Liquids and Solids: Chemical Applications*. NATO ASI Series C – Vol. 322. Dordrecht, Netherlands: Kluwer Academic Publishers; 1990:409-424.

19. Bryce DL, Bernard GM, Gee M, Lumsden MD, Eichele K, Wasylishen RE. Practical aspects of modern routine solid-state multinuclear magnetic resonance spectroscopy: one-dimensional experiments. *Can J Anal Sci Spect*. 2001;46:46-82.

20. Van Vleck JH. The dipolar broadening of magnetic resonance lines in crystals. *Phys Rev*. 1948;74:1168-1183.

21. Pyykkö P. Year-2008 nuclear quadrupole moments. *Mol Phys*. 2008;106:1965-1974.

22. Zax DB, Bielecki A, Zilm KW, Pines A, Weitekamp DP. Zero field NMR and NQR. *J Chem Phys*. 1985;83:4877-4905.

23. Widdifield CM, Perras FA, Bryce DL. Solid-state $^{185/187}$Re NMR and GIPAW DFT study of perrhenates and $Re_2(CO)_{10}$: chemical shift anisotropy, NMR crystallography, and a metal-metal bond. *Phys Chem Chem Phys*. 2015;17:10118-10134.

24. Perras FA, Widdifield CM, Bryce DL. QUEST – QUadrupolar Exact SofTware: A fast graphical program for the exact simulation of NMR and NQR spectra for quadrupolar nuclei. *Solid State Nucl Magn Reson*. 2012;45–46:36-44.

25. Beguš S, Jazbinšek V, Pirnat J, Trontelj Z. A miniaturized NQR spectrometer for a multi-channel NQR-based detection device. *J Magn Reson*. 2014;247:22-30.

26. Scharfetter H. An electronically tuned wideband probehead for NQR spectroscopy in the VHF range. *J Magn Reson*. 2016; 271:90-98.

27. Sato-Akaba H. Design and testing of a low impedance transceiver circuit for nitrogen-14 nuclear quadrupole resonance. *Solid State Nucl Magn Reson*. 2014;63–64:30-36.

28. Pecher O, Halat DM, Lee J, Liu Z, Griffith KJ, Braun M, et al. Enhanced efficiency of solid-state NMR investigations of energy materials using an external automatic tuning/matching (eATM) robot. *J Magn Reson*. 2017;275:127-136.

29. Eichele K. *WSolids1 ver. 1.21.3*. Germany: Universität Tübingen; 2015.

30. Abragam A. *The Principles of Nuclear Magnetism*. London: Oxford University Press; 1961.

31. Lowe IJ. Free induction decays of rotating solids. *Phys Rev Lett*. 1959;2:285-287.

32. Gullion T. Introduction to rotational-echo, double-resonance NMR. *Concepts Magn Reson Part A*. 1998;10:277-289.

33. Samason A, Lippmaa E, Pines A. High resolution solid-state N.M.R. Averaging of second-order effects by means of a double-rotor. *Mol Phys*. 1988;65:1013-1018.

34. Samoson A, Pines A. Double rotor for solid-state NMR. *Rev Sci Instrum*. 1989;60:3239-3241.

35. Frydman L, Chingas GC, Lee YK, Grandinetti PJ, Eastman MA, Barrall GA, et al. Variable-angle correlation spectroscopy in solid-state nuclear magnetic resonance. *J Chem Phys*. 1992;97:4800-4808.

36. Wang SH, Xu Z, Baltisberger JH, Bull LM, Stebbins JF, Pines A. Multiple-quantum magic-angle spinning and dynamic-angle spinning NMR spectroscopy of quadrupolar nuclei. *Solid State Nucl Magn Reson*. 1997;8:1-16.

37. Frydman L, Harwood JS. Isotropic Spectra of Half-Integer Quadrupolar Spins from Bidimensional Magic-Angle Spinning NMR. *J, Am, Chem, Soc*. 1995;117:5367-5368.

38. Rossini AJ, Hanrahan MP, Thuo M. Rapid acquisition of wideline MAS solid-state NMR spectra with fast MAS, proton detection, and dipolar HMQC pulse sequences. *Phys Chem Chem Phys*. 2016;18:25284-25295.

39. Eichele K, Wasylishen RE, Grossert JS, Olivieri AC. The Influence of Chlorine-Carbon Dipolar and Indirect Spin-Spin Interactions on High-Resolution Carbon-13 NMR Spectra of Chloroketosulfones in the Solid State. *J Phys Chem*. 1995;99:10110-10113.

40. Siegel R, Nakashima TT, Wasylishen RE. Signal-to-Noise Enhancement of NMR Spectra of Solids Using Multiple-Pulse Spin-Echo Experiments. *Concepts Magn Reson*. 2005;26A:62-77.

41. O'Dell LA, Schurko RW. QCPMG Using Adiabatic Pulses for Faster Acquisition of Ultra-Wideline NMR Spectra. *Chem Phys Lett*. 2008;464:97-102.

42. Massiot D, Farnan I, Gautier N, Trumeau D, Trokiner A, Coutures JP. ^{71}Ga and ^{69}Ga nuclear magnetic resonance study of β-Ga_2O_3: resolution of four- and six-fold coordinated Ga sites in static conditions. *Solid State Nucl Magn Reson*. 1995;4:241-248.

43. O'Dell LA, Rossini AJ, Schurko RW. Acquisition of ultra-wideline NMR spectra from quadrupolar nuclei by frequency stepped WURST-QCPMG. *Chem Phys Lett*. 2009;468:330-335.

44. Schurko RW. Ultra-Wideline Solid-State NMR Spectroscopy. *Acc Chem Res*. 2013;46:1985-1995.

45. Szell PMJ, Bryce DL. ^{35}Cl solid-state NMR and computational study of chlorine halogen bond donors in single-component crystalline chloronitriles. *J Phys Chem C*. 2016;120:11121-11130.

46. Perras FA, Bryce DL. Direct investigation of covalently bound chlorine in organic compounds by solid-state ^{35}Cl NMR spectroscopy and exact spectral line-shape simulations. *Angew Chem Int Ed*. 2012;51:4227-4230.

47. Szell PMJ, Bryce DL. Recent advances in Chlorine, Bromine, and Iodine solid-state NMR spectroscopy. *Annu Rep NMR Spectrosc*. 2015;84:115-165.

48. Widdifield CM, Chapman RP, Bryce DL. Chlorine, Bromine, and Iodine Solid-State NMR Spectroscopy. *Annu Rep NMR Spectrosc*. 2009;66:195-326.

49. Mandal S, Song Y-Q. Two-dimensional NQR using ultra-broadband electronics. *J Magn Reson*. 2014;240:16-23.

50. Osán TM, Cerioni LMC, Forguez J, Ollé JM, Pusiol DJ. NQR: From imaging to explosives and drugs detection. *Physica B*. 2007;389:45-50.

51. Smith JAS, Rowe MD, Althoefer K, Peirson NF, Barras J. ^{14}N NQR, relaxation and molecular dynamics of the explosive TNT. *Solid State Nucl Magn Reson*. 2015;71:61-66.

52. Barras J, Murnane D, Althoefer K, Assi S, Rowe MD, Poplett IJF, et al. Nitrogen-14 nuclear quadrupole resonance spectroscopy: a promising analytical methodology for medicines authentication and counterfeit antimalarial analysis. *Anal Chem*. 2013;85:2746-2753.

53. Tycko R, Opella SJ. High-resolution ^{14}N overtone spectroscopy: an approach to natural abundance nitrogen NMR of oriented and polycrystalline systems. *J Am Chem Soc*. 1986;108:3531-3532.

54. O'Dell LA, Ratcliffe CI. ^{14}N magic angle spinning overtone NMR spectra. *Chem Phys Lett*. 2011;514:168-173.

55. O'Dell LA, Brinkmann A. ^{14}N Overtone NMR spectra under magic angle spinning: experiments and numerically exact simulations. *J Chem Phys*. 2013;138:064201.

56. Veinberg SL, Lindquist AW, Jaroszewicz MJ, Schurko RW. Practical considerations for the acquisition of ultra-wideline ^{14}N NMR spectra. *Solid State Nucl Magn Reson*. 2017;84:45-58.

57. O'Dell LA, Ratcliffe CI. Ultra-wideline ^{14}N NMR spectroscopy as a probe of molecular dynamics. *Chem Commun*. 2010;46:6774-6776.

58. O'Dell LA, Schurko RW, Harris KJ, Autschbach J, Ratcliffe CI. Interaction tensors and local dynamics in common structural motifs of nitrogen: a solid-state ^{14}N NMR and DFT study. *J Am Chem Soc*. 2011;133:527-546.

59. Harbison GS, Slokenbergs A, Barbara TM. Two-dimensional zero-field nutation nuclear quadrupole resonance spectroscopy. *J Chem Phys*. 1989;90:5292-5298.

60. Sinjavsky N, Ostafin M, Maćkowiak M. Determination of the asymmetry parameter of EFG tensor from moments and NQR nutation spectra in powders. *Appl Magn Reson*. 1998;15:215-225.

61. Bai NS, Reddy N, Ramachandran R. Zeeman-Perturbed Spin-Echo FT NQR Spectroscopy. *J Magn Reson*. 1993;102:137-143.

62. Ramesh KP, Suresh KS, Raghavendra Rao C, Ramakrishna J. Pressure and temperature dependence of the chlorine NQR in caesium and sodium chlorates. *Magn Reson Chem*. 2008;46:525-533.

63. Kushida T, Benedek GB, Bloembergen N. Dependence of the pure quadrupole resonance frequency on pressure and temperature. *Phys Rev*. 1956;104:1364-1377.

64. Bryce DL. NMR crystallography: structure and properties of materials from solid-state nuclear magnetic resonance observables. *IUCrJ*. 2017;4:350-359.

65. Kroeker S, Wasylishen RE, Hanna JV. The structure of solid Copper(I) Cyanide: a multinuclear magnetic and quadrupole resonance study. *J Am Chem Soc*. 1999;121:1582-1590.

66. Rubinstein M, Taylor PC. Nuclear quadrupole resonance in amorphous and crystalline As_2S_3. *Phys Rev B*. 1974;9:4258-4276.

67. Jaroszewicz MJ, Frydman L, Schurko RW. Relaxation-assisted separation of overlapping patterns in ultra-wideline NMR spectra. *J Phys Chem A*. 2017;121:51-65.

68. See http://u-of-o-nmr-facility.blogspot.ca/2008/05/interference-from-fm-radio-stations.html

69. Ludwig GW. Some Bromine, Iodine, and Indium nuclear quadrupole interaction frequencies. *J Chem Phys*. 1956;25:159-171.

70. Web of Science Version 5.25.1. [database online]. Philadelphia, PA: Clarivate Analytics; 2017. www.webofknowledge.com. Accessed August 28th 2017.

71. Rehn V. Covalent-Bond Asymmetries from Zeeman-Split NQR. *J Chem Phys*. 1963;38:749-759.

72. Bucci P, Cecchi P, Colligiani A. The Zeeman Effect of Nuclear Quadrupole Resonance in Single Crystals of Sodium Bromate and p-Dibromobenzene. *J Am Chem Soc*. 1964;86:2513-2514.

73. Schawlow AL. Nuclear Quadrupole Resonances in Solid Bromine in Iodine Compounds. *J Chem Phys*. 1954;22:1211-1214.

74. Hinchliffe A, Munn RW, Pritchard RG, Spicer CJ. The Structure of a Solution-Grown Crystal of 1,4-Diiodobenzene. *J Mol Struct*. 1985;130:93-96.